Figure S1. Deletion of RASA1in BEC during embryonic development results in lethality. *rasa1*$^{fl/+}$ *tie1-cre* mice were bred with *rasa1*$^{fl/fl}$ mice. (**A**) Shown is the number of progeny of the indicated genotypes. Note the absence of *rasa1*$^{fl/fl}$ *tie1-cre* pups. (**B**) *rasa1*$^{fl/fl}$ *tie1-cre* mice succumb at E10.5 of development. Death is associated with the development of cardiovascular abnormalities. Note the distended pericardial sac in the *rasa1*$^{fl/fl}$ *tie1-cre* embryo (arrow).

Figure S2. Expression of VEGFR3 on lymphatic vessels in induced RASA1-deficient mice. Chest wall sections from *rasa1*$^{fl/fl}$ *ub-ert2cre* mice administered TM 3 mo beforehand (at age 2 mo) were stained with anti-LYVE-1 (green) and anti-VEGFR3 (red) antibodies (X 400). Note expression of VEGFR3 upon LV (white arrows) but not BV (blue arrows) revealed in individual and merged images.

Figure S3. Longitudinal imaging of dermal lymphatic vessel flow in induced RASA1-deficient mice. Shown are representative images of ICG flow in a single *rasa1*$^{fl/fl}$ *ub-ert2cre* mouse. Images were taken before and at the indicated number of weeks after TM administration (injected at age 2 mo) and show ICG fluorescence 5 min after ICG injection. LV abnormalities are detected as soon as soon as 2 wk after TM. Similar results have been obtained with five other *rasa1*$^{fl/fl}$ *ub-ert2cre* mice.

Figure S4. Cell surface marker expression upon LEC from induced RASA1-deficient mice. LEC were purified from lungs of TM-treated *rasa1*$^{fl/fl}$ *ub-ert2cre* and *rasa1*$^{fl/fl}$ mice (treated 2 wk beforehand at 2 mo of age) by positive selection using an anti-podoplanin

antibody. (**A**) Shown is expression of CD31 and podoplanin (top), VEGFR-3 and Ep-CAM upon cultured LEC (bottom). Note comparable expression of VEGFR3 and absence of Ep-CAM upon LEC from both mice. (**B**) Western blots showing PDGFR and RASA1 expression levels in purified LEC. Blots were reprobed with a GAPDH antibody to demonstrate equivalent protein loading. Note comparable PDGFR expression upon LEC and near absence of RASA1 in LEC from *rasa1*$^{fl/fl}$ *ub-ert2cre* mice.

Figure S5. Ras signal transduction in induced RASA1-deficient BEC and fibroblasts. BEC and fibroblasts were isolated from lung and tail respectively of *rasa1*$^{fl/fl}$ *ub-ert2cre* and *rasa1*$^{fl/fl}$ mice treated with TM 2 wk beforehand (at 2 mo of age). (**A**) Western blots showing expression of RASA1 in BEC and fibroblasts. Blots were reprobed with a GAPDH antibody to demonstrate equivalent protein loading. (**B**) BEC and LEC were stimulated with the indicated growth factors for the indicated times (in min). Activation of ERKs and AKT was determined by Western blotting with phospho-specific antibodies. Blots were reprobed with ERK and AKT antibodies to demonstrate equivalent protein loading. Experiments have been repeated at least three times with the same results.

Supplemental Videos 1 and 2. NIR fluorescence imaging of dynamic lymph flow in induced RASA1-deficient mice. Shown are videos of ICG flow in TM-treated *rasa1*$^{fl/fl}$ *ub-ert2cre* (video 1) and littermate *rasa1*$^{fl/fl}$ (video 2) mice from Figure 4 from the time of ICG injection until 100 s post-injection.

Supplemental Videos 3 and 4. NIR fluorescence imaging of dynamic lymph flow in LEC-specific induced RASA1-deficient mice. Shown are videos of ICG flow in TM-treated *rasa1*$^{fl/fl}$ *prox1-ert2cre* (video 3) and littermate *rasa1*$^{fl/fl}$ (video 4) mice from Figure 7 from the time of ICG injection until 120 s post-injection.

Supplemental Videos 5 and 6. NIR fluorescence imaging of dynamic lymph flow in induced RASA1-deficient mice treated with a blocking anti-VEGFR-3 antibody. Shown are videos of ICG flow in TM-treated *rasa1*$^{fl/fl}$ *ub-ert2cre* mice (video 5) and TM-treated anti-VEGFR3-treated *rasa1*$^{fl/fl}$ *ub-ert2cre* mice (video 6) mice from Figure 10 from the time of ICG injection until 100 s post-injection.

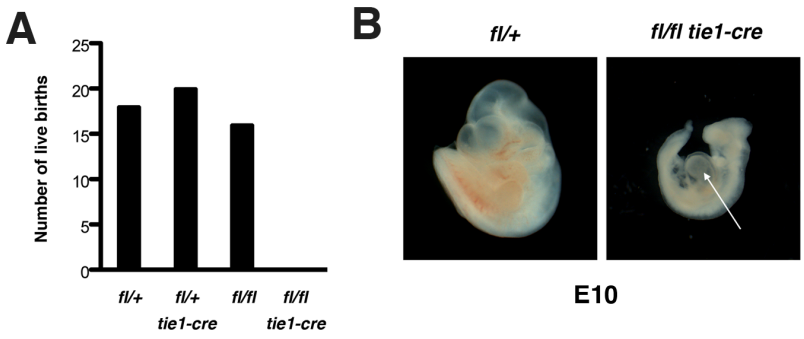

Figure S1. Deletion of RASA1in BEC during embryonic development results in lethality. *rasa1*$^{fl/+}$ *tie1-cre* mice were bred with *rasa1*$^{fl/fl}$ mice. (**A**) Shown is the number of progeny of the indicated genotypes. Note the absence of *rasa1*$^{fl/fl}$ *tie1-cre* pups. (**B**) *rasa1*$^{fl/fl}$ *tie1-cre* mice succumb at E10.5 of development. Death is associated with the development of cardiovascular abnormalities. Note the distended pericardial sac in the *rasa1*$^{fl/fl}$ *tie1-cre* embryo (arrow).

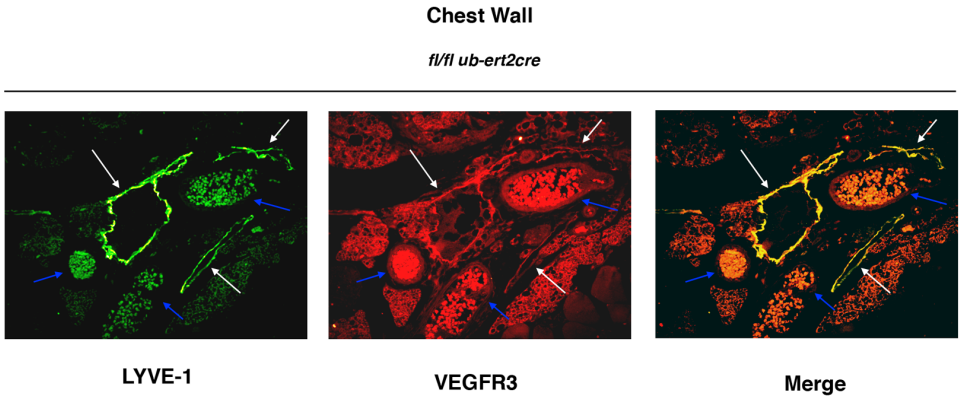

Figure S2. Expression of VEGFR3 on lymphatic vessels in induced RASA1-deficient mice. Chest wall sections from *rasa1*$^{fl/fl}$ *ub-ert2cre* mice administered TM 3 mo beforehand (at age 2 mo) were stained with anti-LYVE-1 (green) and anti-VEGFR3 (red) antibodies (X 400). Note expression of VEGFR3 upon LV (white arrows) but not BV (blue arrows) revealed in individual and merged images.

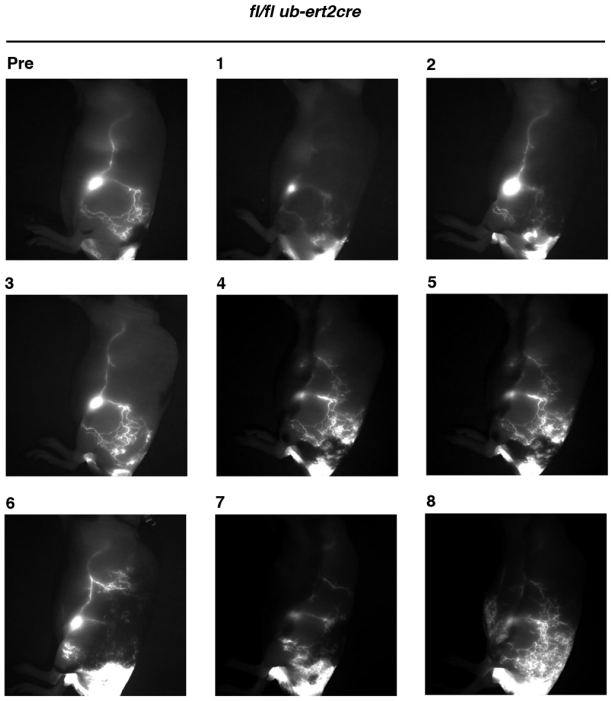

Figure S3. Longitudinal imaging of dermal lymphatic vessel flow in induced RASA1-deficient mice. Shown are representative images of ICG flow in a single *rasa1*$^{fl/fl}$ *ub-ert2cre* mouse. Images were taken before and at the indicated number of weeks after TM administration (injected at age 2 mo) and show ICG fluorescence 5 min after ICG injection. LV abnormalities are detected as soon as soon as 2 wk after TM. Similar results have been obtained with five other *rasa1*$^{fl/fl}$ *ub-ert2cre* mice.

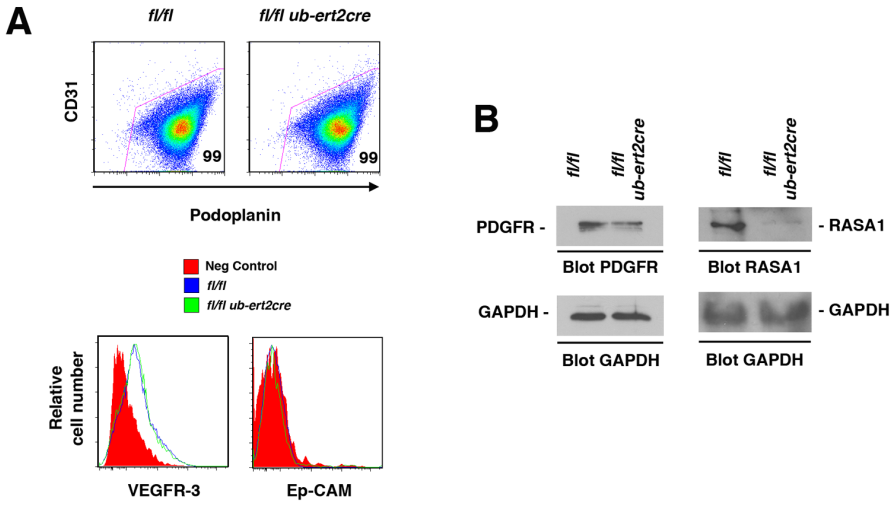

Figure S4. Cell surface marker expression upon LEC from induced RASA1-deficient mice. LEC were purified from lungs of TM-treated *rasa1*$^{fl/fl}$ *ub-ert2cre* and *rasa1*$^{fl/fl}$ mice (treated 2 wk beforehand at 2 mo of age) by positive selection using an anti-podoplanin antibody. (**A**) Shown is expression of CD31 and podoplanin (top), VEGFR-3 and Ep-CAM upon cultured LEC (bottom). Note comparable expression of VEGFR3 and absence of Ep-CAM upon LEC from both mice. (**B**) Western blots showing PDGFR and RASA1 expression levels in purified LEC. Blots were reprobed with a GAPDH antibody to demonstrate equivalent protein loading. Note comparable PDGFR expression upon LEC and near absence of RASA1 in LEC from *rasa1*$^{fl/fl}$ *ub-ert2cre* mice.

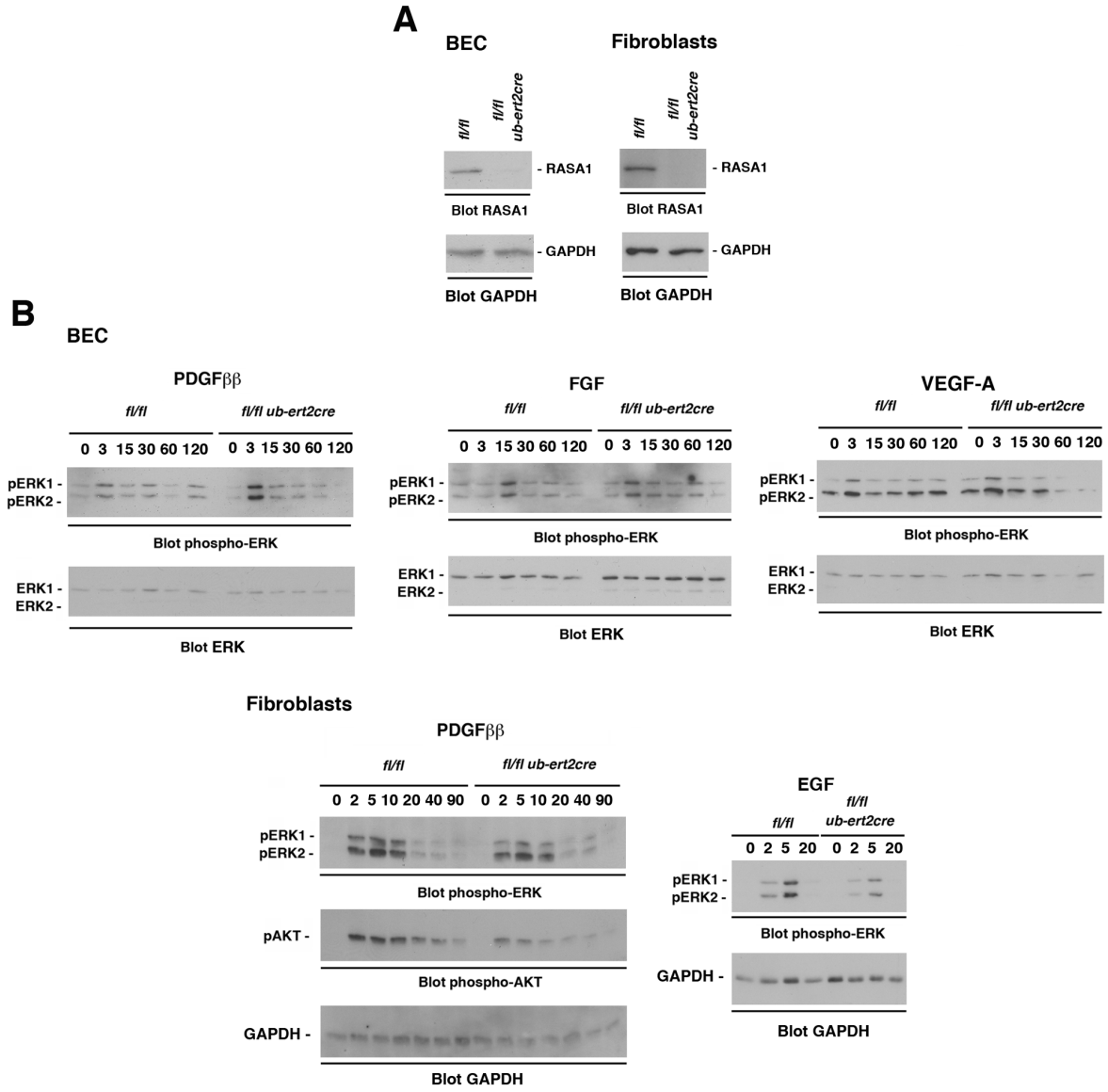

Figure S5. Ras signal transduction in induced RASA1-deficient BEC and fibroblasts. BEC and fibroblasts were isolated from lung and tail respectively of *rasa1*$^{fl/fl}$ *ub-ert2cre* and *rasa1*$^{fl/fl}$ mice treated with TM 2 wk beforehand (at 2 mo of age). (**A**) Western blots showing expression of RASA1 in BEC and fibroblasts. Blots were reprobed with a GAPDH antibody to demonstrate equivalent protein loading. (**B**) BEC and LEC were stimulated with the indicated growth factors for the indicated times (in min). Activation of ERKs and AKT was determined by Western blotting with phospho-specific antibodies. Blots were reprobed with ERK and AKT antibodies to demonstrate equivalent protein loading. Experiments have been repeated at least three times with the same results.